Scientific Research Publishing

Open Journal of Air Pollution, 2026, 15(3), 129-153
https://www.scirp.org/journal/ojap
ISSN Online: 2169-2661
ISSN Print: 2169-2653

Saharan Dust Event over the Gulf of Mexico States and Its Impact on Air Quality in the Summer of 2020

Sergio Natan González-Rocha[1*], Rodolfo Sosa Echeverría[2], Raúl Enrique Contreras Bermúdez[1], Lizeth Ríos Velasco[1], Gilberto Fuentes García[3], Juan Cervantes-Pérez[4], Armando Aguilar-Meléndez[5], Guadalupe Bauza Mendoza[1]

[1]Facultad de Ciencias Químicas, Universidad Veracruzana, Poza Rica de Hidalgo, México
[2]Instituto de Ciencias de la Atmósfera y Cambio Climático-Universidad Nacional Autónoma de México, Ciudad de México, México
[3]Facultad de Ingeniería-Ingeniería Ambiental, Universidad Nacional Autónoma de México, Ciudad de México, México
[4]Licenciatura de Ciencias Atmosféricas, Universidad Veracruzana, Xalapa, México
[5]Facultad de Ingeniería Civil, Universidad Veracruzana, Poza Rica de Hidalgo, Veracruz, México
Email: *ngonzalez@uv.mx, rodsosa@unam.mx, raucontreras@uv.mx, lrios@uv.mx, gilfgar@comunidad.unam.mx, jcervantes@uv.mx, armaguilar@uv.mx, gbauza@uv.mx

How to cite this paper: González-Rocha, S.N., Sosa Echeverría, R., Contreras Bermúdez, R.E., Ríos Velasco, L., Fuentes García, G., Cervantes-Pérez, J., Aguilar-Meléndez, A. and Bauza Mendoza, G. (2026) Saharan Dust Event over the Gulf of Mexico States and Its Impact on Air Quality in the Summer of 2020. *Open Journal of Air Pollution*, **15**, 129-153.
https://doi.org/10.4236/ojap.2026.153008

Received: May 27, 2026
Accepted: September 15, 2026
Published: September 18, 2026

Copyright © 2026 by author(s) and Scientific Research Publishing Inc.
This work is licensed under the Creative Commons Attribution International License (CC BY 4.0).
http://creativecommons.org/licenses/by/4.0/

Open Access

Abstract

The Saharan Dust (SD) is a phenomenon that annually transports dust particles over the Mexican coasts of the Gulf of Mexico. This article analyzes its transport in the summer of 2020 and its effects on air quality. The methodology considered backward trajectories with HYSPLIT, meteorological information from the National Meteorological Service and the National Commission of Water (CONAGUA, Spanish acronym), satellite images, and air quality information from the SINAICA database (SINAICA, Spanish acronym). A combination of mesoscale cyclonic and turbulent systems in the Gulf of Mexico and the north of the country was found. The transport phenomenon occurred over states in the Gulf of Mexico, reaching as far as the state of Nuevo Leon. The HYSPLIT analysis confirmed a trajectory from Africa, with winds from 3000 to 5000 m AGL over Africa and descending to 50 m AGL in Mexico. Air quality stations of Yucatan, Veracruz, and Nuevo Leon show increases in particle concentrations, reaching values around 50 μg/m^3. The $PM_{2.5}$ and PM_{10} concentrations evaluated contributed to effects on air quality, generating quality indices from poor to extremely poor according to concentrations recorded and analyzed at stations in the state of Veracruz. In future research, it is planned to analyze SD using elemental analysis techniques and its impact on human health.

Keywords

Saharan Dust, Dust Transport, Desert Dust, HYSPLIT, $PM_{2.5}$, PM_{10}, Gulf of Mexico, ENSO

1. Introduction

SD is observed in regions near Africa, such as the Mediterranean coast, Europe, and Asia. The characteristics of the dust, as well as the rotation and circulation of the winds on Earth, promote its transport to distant regions, crossing, for example, the Atlantic to the Americas from Africa. Studies and measurement campaigns on the arrival of SD [1] have been carried out in the Yucatan Peninsula and in cities in the Caribbean. SD contributes to poor air quality because of transport events from the Sahara Desert. This transport usually occurs between June and July, corresponding to summer winds. In addition, low-altitude jet currents (Saharan Air Layer) promote their arrival in the Mexican Caribbean region and the Yucatan Peninsula. The ENSO at the end of 2020 could be a synoptic driver of conditions on the sea surface and in the air temperature over the Atlantic, Caribbean, and the Gulf of Mexico [2].

Ramírez-Romero *et al.* [1] used particles smaller than 10 micrometers (PM_{10}) as an indicator. Also, satellite observations from MERRA-2 (Version 2 of the Modern-Era Retrospective Analysis for Research and Applications) were used to estimate the concentration of particles arriving on Mexican soil. In this regard, increases in particle concentrations were observed using satellite data. The origin of the Saharan desert dust was also analyzed using retro-trajectory techniques. Harr *et al.* [3] compared the effects of the 2020 and 2015 events of African Dust. Kaskaoutis *et al.* [4] analyze the weather conditions and the main pathways and transport mechanisms that favor the presence of specific aerosol types over Athens, Greece. Three main aerosol types were identified (urban/industrial, UI; clean maritime, CM; and desert dust, DD), each one corresponding to different optical characteristics and source regions. Aerosol optical depth at 550 nm (AOD550) and fine mode (FM) values from a Terra-MODIS dataset in the period 2000-2005 were used. Pateraki *et al.* [5] reported 127 daily parallel measurements of PM_{10}, $PM_{2.5}$, and PM_1 across the Athens basin in warm and cold periods of the year, while obtaining a more detailed picture of the NO_x and O_3 pollution problems. Pollutant data were taken into consideration. Also, a CAMx simulation was performed.

Prospero and Mayol-Bracero [6] describe some elements found in their study, such as iron (Fe), phosphorus (P), and compounds that acidify rain and soil in the study region. The health impacts implied by the estimated and measured concentrations of these compounds are also discussed. In summer, they observed a higher incidence and seasonal transport of dust in contrast to winter, which shows minimal concentrations. Garrison *et al.* [7] describe their findings related to persistent organic compounds (POPs), metals, and microbes transported to the Caribbean.

Graciela *et al.* [8] describe how African Dust and biomass burning affected Yucatan from 2017 to 2018. Córdoba *et al.* [9] found ice-nucleating particles over the Yucatan Peninsula and their effects on aerosol particles. Different studies in Europe analyzed the composition of the SD and their correlation with synoptic and mesoscale meteorology [10]-[13].

Dimitriou and Kassomenos [14] describe in their study on Greece the analysis of the SD event that occurred in April 2008, which deteriorated the air quality in Athens and caused decreased visibility. Some elements found from the transport of SD in areas of Italy, the central Mediterranean, and Spain were calcium (Ca), silicon (Si), titanium (Ti), magnesium (Mg), and iron (Fe) [13] [15]-[17] Transport events in the Mediterranean of SD have been identified in the periods of spring, summer, and early autumn. Effects of PMCOARSE material (PM_{10} + $PM_{2.5}$) on health and mortality are related to cardiovascular and respiratory diseases, mainly in Spain and Italy, among others.

Samoli *et al.* [18] assessed the short-term effects of particulate matter with aerodynamic diameter < 10 μg/m^3 (PM_{10}), sulfur dioxide (SO_2), nitrogen dioxide (NO_2), and ozone (O_3) on pediatric asthma emergency admissions in Athens, Greece, over the period 2001-2004. The study confirms previously reported PM_{10} effects on emergency hospital admissions for pediatric asthma and further provides evidence of stronger effects during desert dust days. Tobías *et al.* [19] evaluated the relationship between particulate matter and daily mortality, which has recently been addressed in studies conducted in Southern Europe; they found evidence of stronger adverse health effects of PM_{10} and $PM_{2.5}$ during SD outbreaks for impacted European populations, but not for $PM_{2.5}$.

Some researchers use aerosol optical depth (AOD) and ground-based particulate matter (PM) monitoring station observations to quantify dust over the analysis periods. Urrutia-Pereira *et al.* [20] assessed the relationship between exposure to SD and its implications for human health in the Americas [21]. Kaskaoutis *et al.* [22] analyzed an intense SD event that occurred over the Eastern Mediterranean and Greece on 16-17 April 2005 using satellite observations and ground-based measurements. In April 2005, three dust events were identified above the area, strongly influencing the aerosol load and the PM_{10} concentrations on the surface. Both Terra- and Aqua-MODIS sensors indicated the dust outflows. Remoundaki *et al.* [23] focus on the contribution of SD to PM_{10} levels at an urban site in large Southern European cities, which became a priority during the last decade.

Information from MODIS and TERRA has been used to visualize satellite images, the use of LIDAR for aerosol measurement, software such as R and HYSPLIT for backward trajectory analysis, and the thermal stress index and air quality have also been estimated. The transport of SD over the Gulf of Mexico has also been modeled in 2D [15] [24]-[29]. Bi *et al.* [30] describe this event as a massive global transport of African dust with impacts on the remote atmosphere.

Few studies have been conducted in other regions of the country of Mexico, so

this work aims to analyze the unusual event of the transport of this SD, which was transported to other areas of Mexico. The main objective is to analyze the contributions of PM_{10} that occurred in the weeks between June 22 and July 12, 2020, in the states of Veracruz, Nuevo Leon, and Yucatan, as well as the impact on air quality in the state of Veracruz. To achieve this, an evaluation of data from observations of PM_{10} and $PM_{2.5}$ particles from the National Air Quality Information System (SINAICA) of the National Institute of Ecology and Climate Change (INECC, Spanish acronym) will be carried out within the analysis period. Using the HYSPLIT system, a backward-trajectory analysis will be carried out to determine the movement of dust from the Sahara in Mexico. Finally, atmospheric movements will be reviewed by analyzing meteorological information from the National Meteorological Service of the National Water Commission (SMN-CONAGUA, Spanish acronym) and satellite image information from NASA®'s Worldview website [31].

2. Methodology

2.1. Study Area and Description

The methodology of the investigation considered the selection of the study site by the identification of natural, fixed, and mobile sources. The analysis period was also chosen due to the PM_{10} and $PM_{2.5}$ particle observations from the National Air Quality Information System (SINAICA) of the INECC. As mentioned in their work [1], the annual arrival trajectories to Mexico pass through the Caribbean, cross the Yucatan Peninsula, and extend through the Gulf of Mexico. Figure 1 shows the area over the Gulf of Mexico.



Figure 1. Gulf of Mexico and selected states. Source: Authors.

2.2. Selection of Days and Years of Events

The delimitation of the analysis window of the event considered previous studies conducted in Mexico. These studies indicated that during May to July months, there is historically an influx of Saharan dust reaching Mexico. As a second criterion, satellite imagery analysis was performed and showed that during these periods, the transport of the SD was more intense. Finally, this information was corroborated using PM_{10} and $PM_{2.5}$ concentration records obtained from air quality monitoring stations located in the study area [1] [8]. The selection for 2018 and 2019 was considered before the peak event in summer 2020, due to the quantity of AQ data in the SINAICA database.

2.3. HYSPLIT, Meteorological, and Air Quality Information

SD from Africa was modeled using the HYSPLIT system in conjunction with backward trajectory analysis, as well as the altitudes of dust transport from the Sahara Desert to Mexico [32]-[34]. The HYSPLIT configuration considered an ensemble with 3 coordinates derived from the visual analysis of the images of NASA® Worldview, the first starting in the Sahara Desert, Latitude 18.787390 and Longitude −14.001159, a second coordinate in the middle of the Atlantic Ocean, and a third coordinate in the Yucatan Peninsula, Latitude 20.274413 and Longitude −87.733412. The configuration with 15 days of backward trajectories and a level high of 500 m AGL, with 315 hours of analysis, meteorology 0000Z Jun 15 2020 GDAS1. In the Yucatan Peninsula, the configuration considered 200 hours, and in both trajectories, the Model Vertical Velocity was used.

Finally, the methodologies were adapted to analyze meteorological phenomena information from the National Meteorological Service of the National Water Commission (SMN-CONAGUA) and satellite images from the NASA® Worldview website. This assessment allowed the estimation of SD transport. The analysis, estimations, graphs, and evaluation of particle concentrations were made in Excel, with the data downloaded and validated from SINAICA, all of this supported by information from the selected air quality information ground stations over the Gulf of Mexico [15] [24]-[29].

The current Mexican air quality index, called the "Air and Health Quality Index" (AHQI), considers various regulations from the Ministries of Health and Environment. The Mexican standard NOM-025-SSA1-2014 establishes the reference frameworks for PM_{10} and $PM_{2.5}$ pollutants, which are established in accordance with it, as shown in **Table 1**.

Table 1. PM_{10} and $PM_{2.5}$ calculation bases.

Pollutant	Base concentration
PM_{10}	12-hour weighted moving average concentration
$PM_{2.5}$	Significant digits 0

Source: NOM-172-SEMARNAT-2014.

NOM-172-SEMARNAT-2019 establishes the process to calculate the 12-hour weighted moving average for PM_{10} and $PM_{2.5.}$ The permissible limit values of the Air and Health Quality Index and the related color are shown in Table 2. The formulas are:

$$\bar{C} = \frac{\sum_{i=1}^{N} C_i W^{i-1}}{\sum_{i=1}^{N} W^{i-1}} \tag{1}$$

$$W = \begin{cases} w & \text{si } w > 0.5 \\ 0.5 & \text{si } w \le 0.5 \end{cases} \text{ and } w = 1 - \frac{C_{\max} - C_{\min}}{C_{\max}} \tag{2}$$

$$\bar{C} = \frac{\sum_{i=1}^{12} C_i W^{i-1}}{\sum_{i=1}^{12} W^{i-1}} \tag{3}$$

where:

$\bar{C}$ = weighted moving average concentration;

N = 12;

Σ = data summation;

C_i = average hourly concentration for hour I;

I = consecutive hour of measurement;

W = weighting factor;

W = weight value;

$C_{\max}$ = maximum hourly average concentration over a 12-hour period;

$C_{\min}$ = minimum hourly average concentration over a 12-hour period.

The calculation was performed in Excel to estimate the concentration in μg/m^3 and to evaluate the effect of SD particles on air quality values.

Table 2. Air and health quality index (AHQI), permissible limits of PM_{10} and $PM_{2.5}$.

AHQI	PM_{10} concentration range 12-hour weighted moving average (μg/m^3)	$PM_{2.5}$ concentration range of 12-hour moving average (μg/m^3)
Good	Up to 50	Up to 25
Acceptable	Over 50 to 75	Greater than 25 up to 45
Bad	Greater than 75 up to 155	Greater than 45 to 79
Very Bad	Greater than 155 to 235	Greater than 79 to 147
Extremely Bad	Greater than 235	Greater than 147

Source: NOM-172-SEMARNAT-2014.

3. Results and Discussions

3.1. Study Area Description

The work focused on the Gulf of Mexico area, including the south, southeast, and northeast of Mexico, considering the states of Yucatan, Veracruz, and Nuevo Leon, due to their proximity to the arrival zone of the SD, which usually comes from the Caribbean annually. Figure 2 shows the selected cities and states in Mexico.

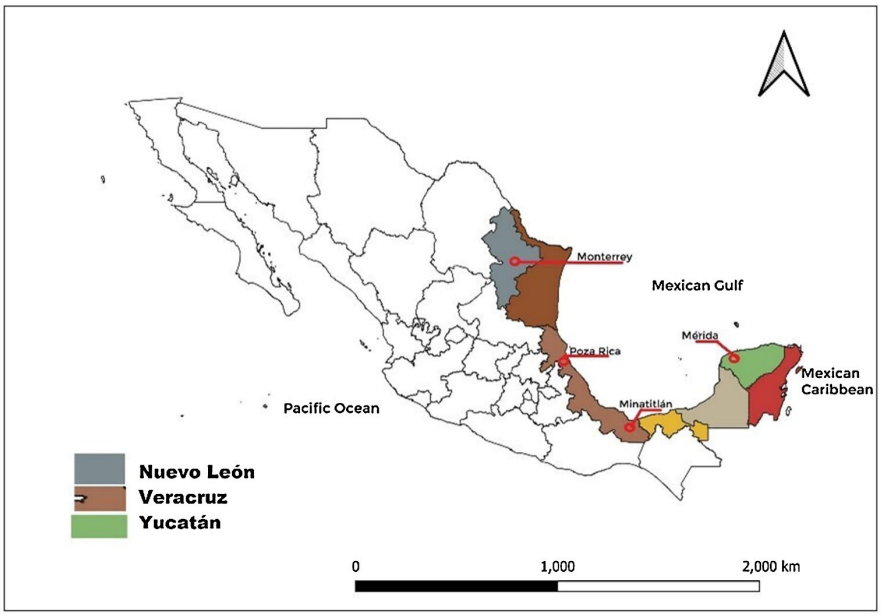


Figure 2. States of the Gulf of Mexico, the Caribbean, and three state cities, where the SD was evaluated in June 2020. Source: Authors.

The states mentioned above are topographically composed of coastal plains and high mountain areas belonging to the Sierra Madre Oriental. The Sierra Madre Oriental extends parallel to the Gulf of Mexico to the south of the State of Veracruz; possibly, this condition promoted the displacement of SD toward the northeast and north of Mexico.

The cities in the states of Yucatan, Veracruz, and Nuevo Leon were selected according to INEGI as metropolitan zones (MZ), as shown in **Table 3**. These cities have road, air, and rail transport in constant movement. There are industrial sources such as a refinery in Minatitlan, a gas processing plant, and oil fields in Poza Rica, all constant sources of particles in the state of Veracruz. In the city of Monterrey, there are industrial and transportation sources because it is the largest MZ of the selected cities. The city of Mérida, due to its constant annual arrival of dust, is the only reference for the intrusions of SD in Mexico.

Table 3. Metropolitan areas with selected air quality stations.

Metropolitan zone (MZ)	State	Population
Monterrey	Nuevo León	5,341,171
Poza Rica	Veracruz	521,530
Coatzacoalcos-Minatitlán	Veracruz	355,738
Mérida	Yucatan	921,771

Source: Prepared by the authors and adapted with information from SINAICA.

Another issue considered in this work was the forest fires that occur in the areas surrounding the selected metropolitan areas, as indicated in the National Forestry

Commission (CONAFOR, Spanish acronym) reports from past years. In the weekly report on forest fires, 120 fires were reported in the state of Veracruz, 44 in the state of Nuevo León, and 26 in the state of Yucatan [35] [36].

3.2. Identification of Natural and Anthropogenic Sources in the Study Area

The database information collected for the analysis of the study area was correlated with forest fire data from the National Council of Forests (CONAFOR, Spanish acronym) and the Secretary of Natural and Marine Resources (SEMARNAT, Spanish acronym) [35] [36]. There were six forest fires in the Veracruz state in mountain regions, not in the SD trajectory in EMCAV1 or EMCAV2.

INEGI's demographic data and pollutant information are from SINAICA. The information was used to assess background particles and the air quality data from ground stations or NASA images. In the prior days, the average ranges registered were from 5.1 to 13.4 mg/m^3 in $PM_{2.5}$ and from 7.7 to 15.9 mg/m^3 in PM_{10} in Poza Rica. In Minatitlan, the averages in PM_{10} were from 12.4 to 16.0 mg/m^3.

3.3. Satellite Image and Backward Trajectory Analysis in HYSPLIT

For the analysis of satellite images, photos available from the NASA Worldview site [31] were downloaded from June 20 to 30 and until July 12. **Figure 3**.

The NOAA HYSPLIT trajectory tracking software [32] [33] was used in selected cities during this event. The system is available online at https://www.ready.noaa.gov/HYSPLIT.php. The HYSPLIT options allow choosing between independent points or spatial arrangements for areas under evaluation. For this process, the cities of Poza Rica and Minatitlan in the state of Veracruz were selected. Mérida in Yucatan and Monterrey in Nuevo León, initially considering the starting coordinates of the retro trajectory. For this purpose, a point was chosen on the coast of Africa in the Sahara desert, an intermediate point over the Atlantic Ocean was chosen due to assessment of the satellite images, and a point over the Yucatan Peninsula was selected to see how far the SD arrived in the states of the Gulf of Mexico in June 2020.

3.4. Evaluation of Synoptic Meteorological Conditions

To assess the synoptic meteorological conditions in the country during the event, the SMN-CONAGUA, the reports corresponding to forecasts 343, 345, 347, 349, 351, 353, and 355 were reviewed. The Meteorological Bulletins of the Regional Hydrometeorological Center in Veracruz, Mexico, summarize the meteorological systems that affected the area. The documents described meteorological events or conditions that could have driven the transport of SD to the northern areas of Mexican territory. Hence, the cities in the state of Veracruz were selected.

Meteorological parameters, when interacting with air quality parameters, create synergistic effects that increase or decrease pollutant concentrations [22] [37]-[41]. These parameters were downloaded from meteorological databases, selecting the variables relative humidity (RH), precipitation (PP), wind speed (WS), and

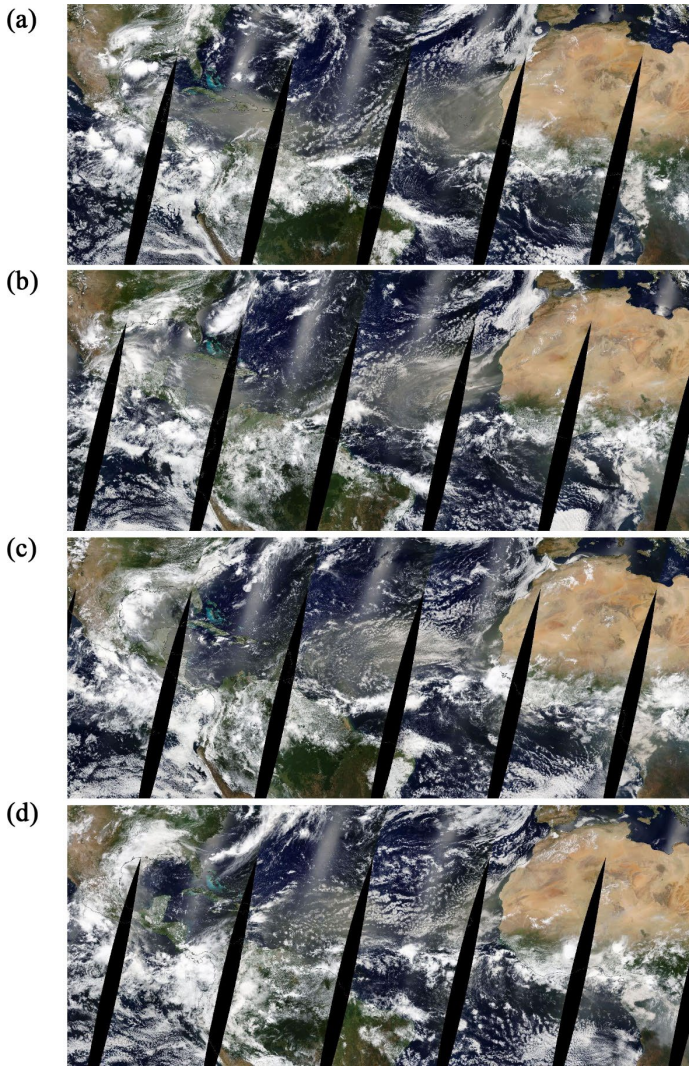


Figure 3. Monitoring the SD event from June 23-26, 2020, over Mexico by means of satellite images from [33] https://worldview.earthdata.nasa.gov/. (a) The arrival of the SD cloud to the southern region of the island of Cuba on June 23, approaching the Caribbean Sea; (b) Image from June 24, the cloud is seen arriving in the Mexican Caribbean over the coasts of Quintana Roo and Central America; (c) On June 25, the SD cloud is seen crossing the Yucatan Peninsula over the states of Quintana Roo, Yucatan, and Campeche, entering the southern Gulf of Mexico; finally, (d) The dust cloud is observed on June 26 over the northeastern part of Mexico over the states of Veracruz, Tamaulipas, and Nuevo León, as well as in part of the Gulf of Mexico on the south-southeastern coast of the United States.

ambient temperature (TA). Some of the most important variables reviewed in this work were correlated with particles and some events that cause disturbances in the results. For the development of the selected parameters of this analysis, the values of mean TA, maximum TA, minimum TA, accumulated PP, RH, and average WS in the evaluated period were considered.

Another meteorological phenomenon known as El Niño Southern Oscillation (ENSO) annually causes changes in global temperature. The 2020 ENSO could have caused a particularly warm year, with increases in global temperatures above

the sea and the air. Hence, it could be a driver of dust transport from the Sahara Desert to the Caribbean and the Gulf of Mexico. Simulations by Zhou *et al.* [2] describe SST anomalies in the central-eastern equatorial Pacific, including strong anomalous southeasterly winds over the southeastern tropical Pacific and the related subsurface thermal anomalies from 1870 to 2021.

3.5. Data Download from the SINAICA INECC Database

A necessary phase to account for the probable dust particles from the Sahara consists of downloading information from the SINAICA air quality databases of the INECC, considering the download of $PM_{2.5}$ and PM_{10} information in the reference periods chosen due to the availability of information and temporal proximity to the event. The years 2018, 2019, and 2020 were considered during the months of the SD transport events above the Gulf of Mexico. The database is available at https://sinaica.inecc.gob.mx/.

3.6. Satellite Image Analysis and Trajectory Analysis Using HYSPLIT

One phase addressing SD involves downloading data from the SINAICA air quality databases of INECC [42], including $PM_{2.5}$ and PM_{10} measurements for selected reference periods, based on data availability and temporal proximity to the event. The analysis considers the years 2018, 2019, and 2020, focusing on the months when SD transport events occurred over the Gulf of Mexico.

NOAA's HYSPLIT trajectory tracking software [32] [33] modeled trajectories with multiple starting points. The results of the dust transport over the Mexican territory during the study period are shown in **Figure 4**.

3.7. Weather Events during the Assessment Period

During the study period, SMN-CONAGUA reported in forecast bulletins 343, 345, 347, 349, 351, 353, and 355 a low-pressure meteorological event related to tropical waves 6, 7, 8, and cold fronts from the north out of season, which are shown in **Figures 5(a)-(d)**. It was observed that these favored the transport of SD over the coasts of the Gulf of Mexico and the national territory. **Table 4** shows that during the event in the cities of the states of Yucatan and Veracruz, a low-pressure system was associated and impelled the particles from the Atlantic Ocean towards Mexican territory. High temperatures were also recorded during this period. These temperatures may have favored transport events due to convection of surrounding air from cold fronts and from the out-of-season north winds that arrived at the Gulf of Mexico coast, and warm temperatures that promoted winds, with dust transport to the incidence area, as observed in **Figures 5(a)-(d)**.

Table 4 summarizes some meteorological parameters of the cities where the study was carried out, due to air quality measurement stations installed, which include measurements of meteorological variables. The parameters of relative humidity (RH), maximum ambient temperature (TA max), minimum (TA min),

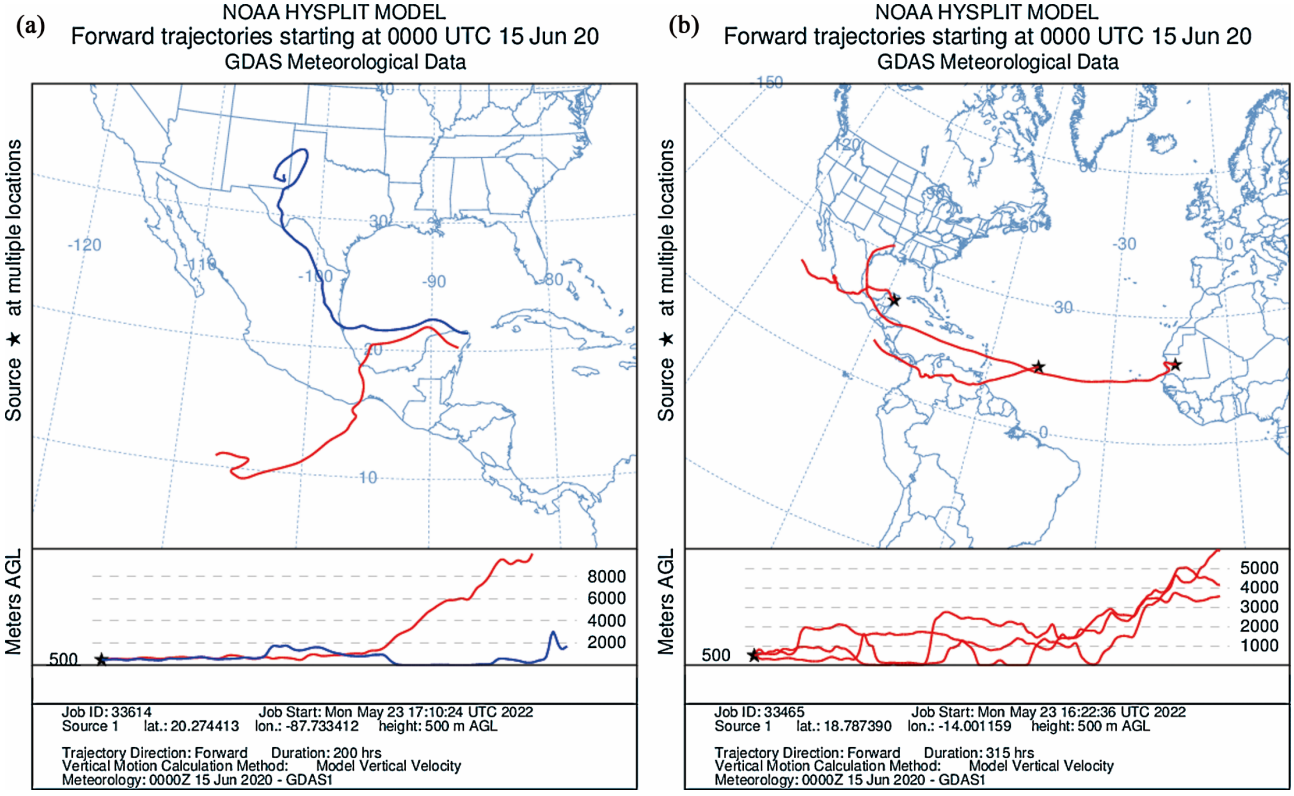


Figure 4. HYPLIT trajectories: (a) Transport from the Sahara Desert, and (b) Considering the Yucatan Peninsula during the analysis period in June 2020. Source: Authors.

Table 4. Average monthly weather data for selected cities for the month of June 2020.

City/State	RH average (%)	TA Max (˚C)	TA Min (˚C)	TA average (˚C)	WS average (km/h)	PP mm
Monterrey/Nuevo Leon	71	35.3	21.6	28.5	12.4	138.3
Poza Rica/Veracruz	75	38	22	30	11	-
Minatitlan/Veracruz	80	36	22	29	14	-
Merida/Yucatan	-	36	14	28	14.6	-

Source: [43] https://www.meteored.mx/.

and average (TA average), wind speed (WS), and precipitation (PP) are important in this dust particle transport phenomenon. In the day-by-day assessment, these parameters undergo variations that cause a decrease in particle concentration, accelerate or remain suspended, or also allow speed variation of the SD transport in the atmosphere. As mentioned in its forecast by SMN-CONAGUA, high temperatures were observed in the daytime environment on the Veracruz coast.

3.8. SINAICA Database

The assessment of the information began with the search for the monthly periods

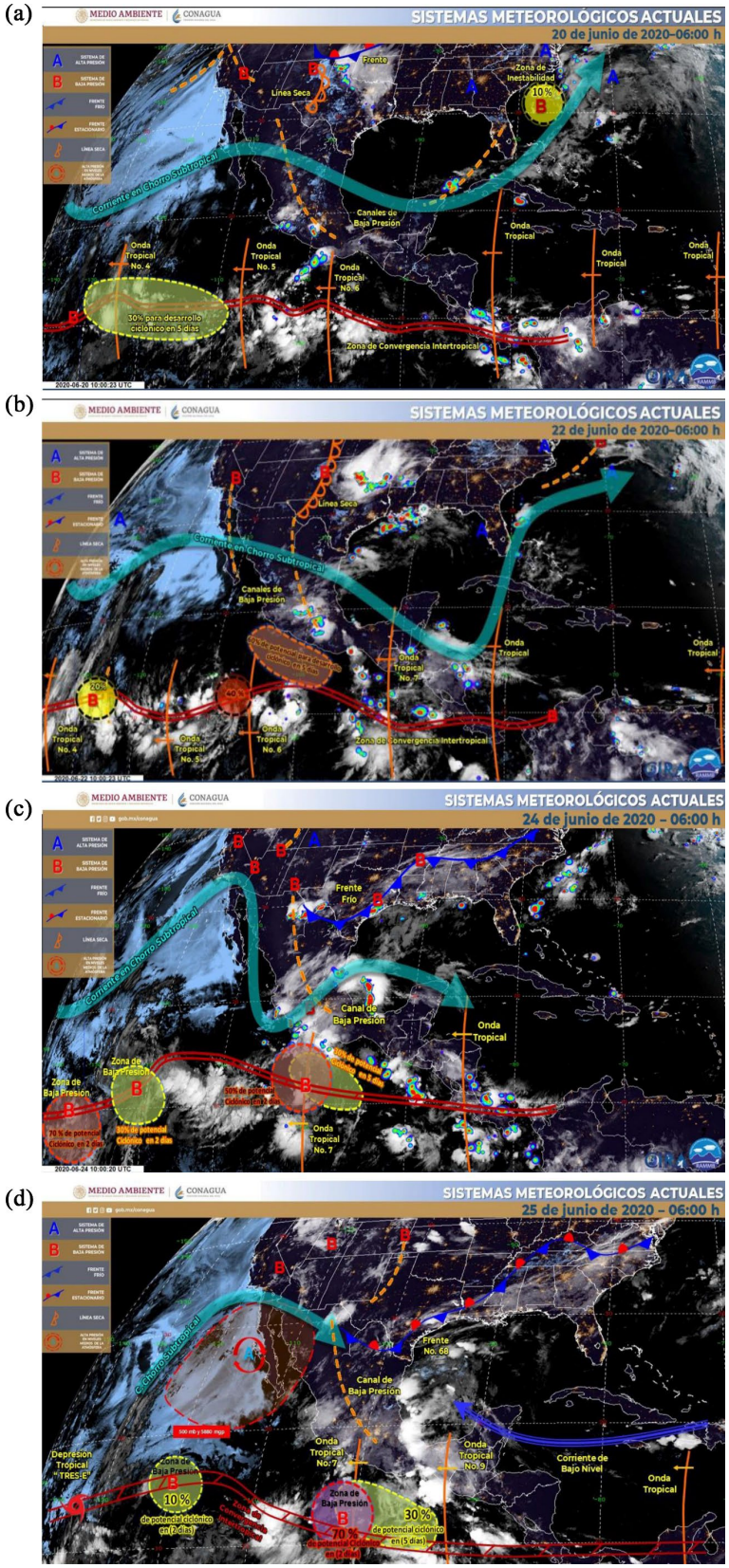


Figure 5. Weather forecast for Mexico from June 20 to 26, daily reports in SMN-CONAGUA, available at https://www.uv.mx/personal/ngonzalez/data_ojap/.

during which the Sahara Desert dust transport phenomena had an impact in reference years from 2018 to 2020. The information on air quality and meteorological parameters was downloaded from the SINAICA website. The AQ measuring stations were selected, and the years 2018, 2019, and 2020 were chosen. The selection of the measuring stations considered the probable transport previously estimated with the HYSPLIT® software, which described the trajectories towards some of the comparison points over the Gulf of Mexico. It is important to mention that the existence of AQ monitoring stations in Veracruz and Yucatan is limited compared to the city of Monterrey. Information from the selected receptor cities and AQ stations is shown in Table 5.

The downloaded files in CSV format were reviewed and validated using the procedure of the INECC atmospheric monitoring manuals [44], the NOM NOM-172-SEMARNAT-2014 and NOM-025-SSA1-2014, criteria for the elimination of negative data from the observations, and verification of whether they cover the standard percentage of at least 75% sufficiency of information from the observations of the month.

Table 5. Selected air quality monitoring stations and receptor coordinates.

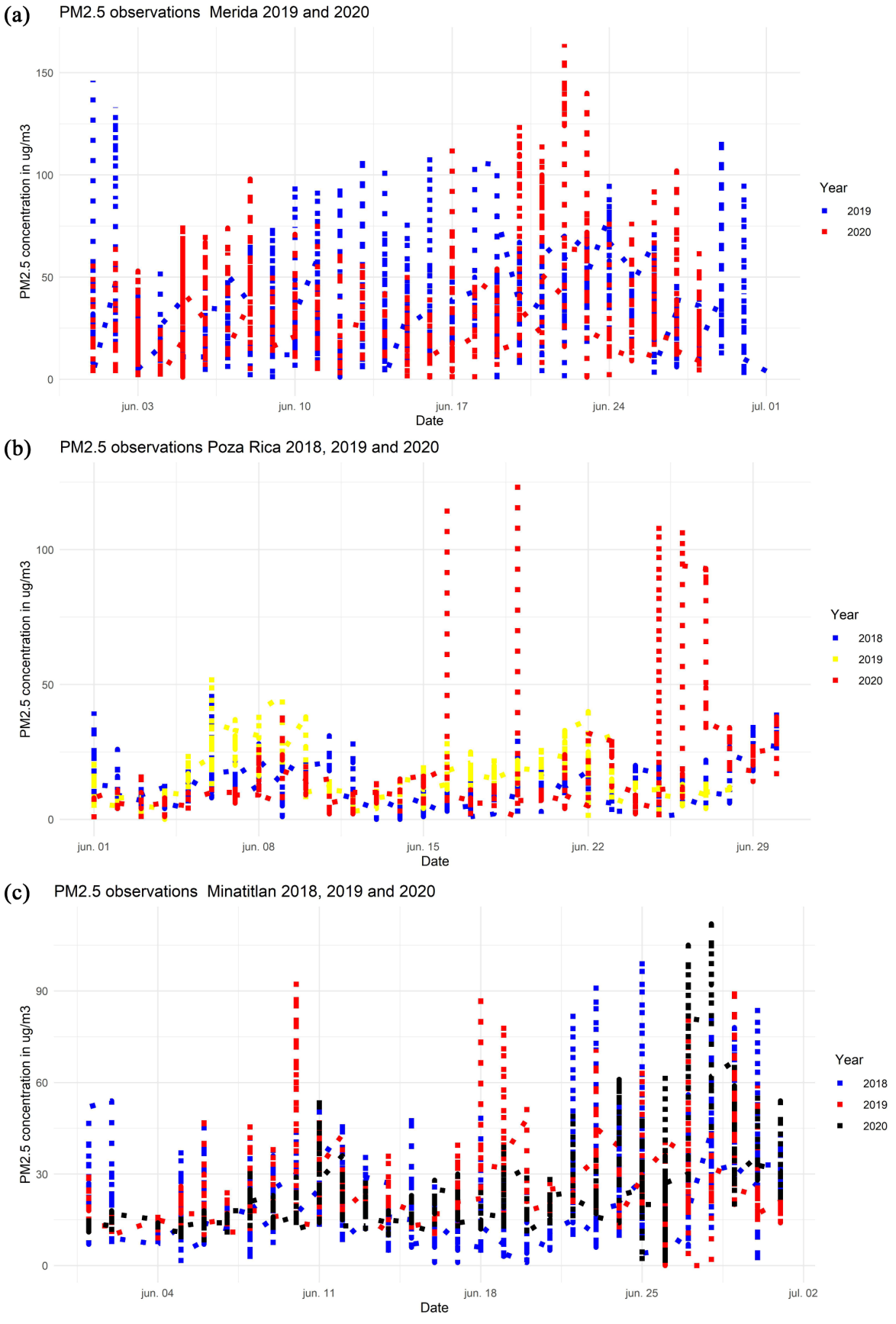
State	City	Station code	Available data	Location latitude/longitude
Nuevo León	Monterrey	EMCAM1 (Universidad)	PM_{10}, $PM_{2.5}$, relative humidity, temperature	25.73 N, 100.31 W
Veracruz	Poza Rica	EMCAV1 (Universidad Veracruzana)	PM_{10}, $PM_{2.5}$, relative humidity, temperature	20.51 N, 97.45 W
Veracruz	Minatitlán	EMCAV2 (Tecnológico)	PM_{10}, $PM_{2.5}$, relative humidity, temperature	18.01 N, 94.56 W
Yucatan	Mérida	EMCAY1 (SDSO1)	PM_{10}, $PM_{2.5}$, relative humidity, temperature	20.97 N, 89.62 W

Source: SINAICA.

3.9. Time Series of Particle Transport PM_{10} and $PM_{2.5}$

The results from the day-by-day analysis of the SD transport event show the recorded particle concentrations from the air quality monitoring stations selected for this work. They are presented below in Figures 6(a)-(d).

In Figure 6(a) at the EMCAY1 station corresponding to the city of Mérida, the entry of SD into Mexico and the concentrations in μg/m^3 were observed during the evaluation period from June 20 to 30; considering the meteorological conditions of the period, the effect of the low-pressure channel and the southern winds coming from the Caribbean area were observed. In general, this area receives the SD from the Caribbean in the Mexican Republic; concentrations of 40.08 and 52.87 μg/m^3 differences on average were observed in the period; there are maximum observations of up to 164.0 μg/m^3 on June 22, compared to those of 100.0


(a)
PM2.5 observations Merida 2019 and 2020
PM2.5 concentration in ug/m3
150
100
50
0
jun. 03
jun. 10
jun. 17
jun. 24
jul. 01
Date
Year
2019
2020
(b)
PM2.5 observations Poza Rica 2018, 2019 and 2020
PM2.5 concentration in ug/m3
100
50
0
jun. 01
jun. 08
jun. 15
jun. 22
jun. 29
Date
Year
2018
2019
2020
(c)
PM2.5 observations Minatitlan 2018, 2019 and 2020
PM2.5 concentration in ug/m3
90
60
30
0
jun. 04
jun. 11
jun. 18
jun. 25
jul. 02
Date
Year
2018
2019
2020

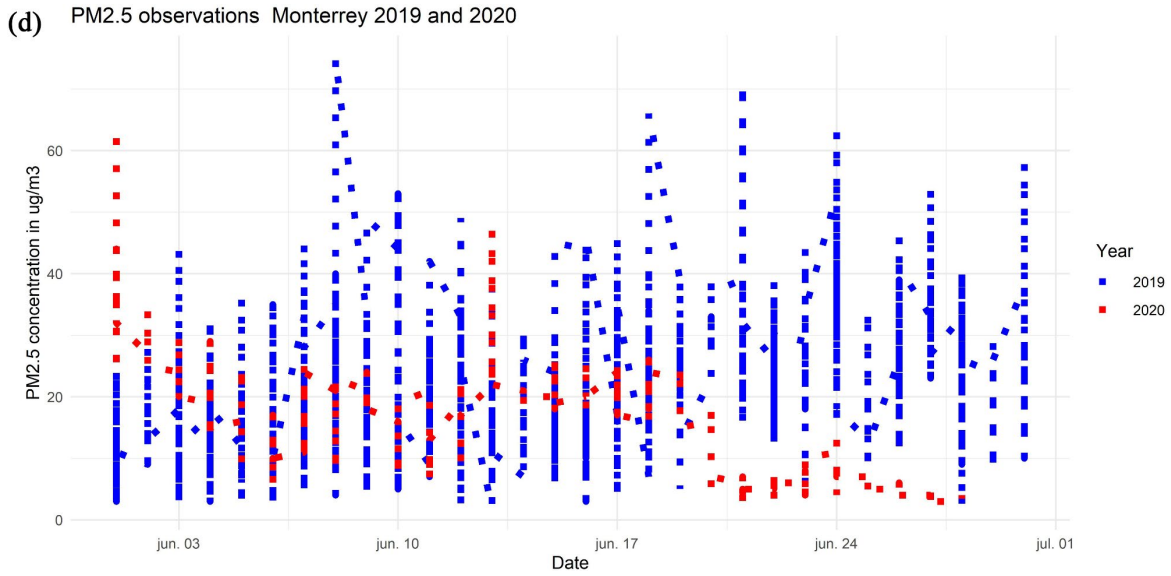


Figure 6. Comparison of concentrations of $PM_{2.5}$ observations at air quality monitoring stations in the cities of (a) Merida (EMCAY1), (b) Minatitlan (EMCAV2), (c) Poza Rica (EMCAV1), and (d) Monterrey (EMCAM1), 2018, 2019 and 2020.

μg/m^3 in 2019. In general, in 2019, it did not exceed 100.0 μg/m^3 of $PM_{2.5}$, unlike in 2020, when in multiple observations it exceeded 100.0 μg/m^3. As mentioned in previous subtopics, factors such as forest fires, vehicular traffic, and proximity to the maritime zone generated various types of particles that may affect the background observations of the area not considered in this work.

Figure 6(b), which corresponds to the EMCAV2 station, shows average observations from 2018 to 2020 of 20.33, 23.65, and 25.33 μg/m^3, respectively; maximum values of 101.0, 93.0, and 112.1 μg/m^3 of $PM_{2.5}$ concentration in 2018, 2019, and 2020; and 80% of the values for 2019 and 2018 were less than 80.0 μg/m^3. This station is in an area where particulate matter typically comes from the industrial zone of "Pemex" and petrochemical companies. It is situated in a metropolitan area with aerosol presence due to its proximity to the Gulf of Mexico coast. As observed in the Hysplit backward trajectory analysis, this area also forms a current crossing the Mexican territory from the Gulf of Mexico to the Pacific Ocean through the Isthmus of Tehuantepec in Oaxaca. This likely facilitated the transport of some particles from the Gulf through this region. However, at altitudes below 4000 meters above ground level (AGL), the trajectory moves toward the northern part of the state, which is associated with the images from the SMN-CONAGUA forecast, as shown in Figure 4 and Figure 5.

Figure 6(c), corresponding to the EMCAV1 station, clearly shows an increase in $PM_{2.5}$ particles compared to the years 2018 and 2019; values less than 40.0 μg/m^3 were observed in the years 2018 and 2019, compared to the year 2020, which presents values higher than 60.0 μg/m^3, reaching maximun of up to 110.0 μg/m^3. In this station, during the analysis period, a meteorological system was detected with high temperatures and a cyclonic system that promoted transport over the MZ of

Poza Rica during the period from June 26.0 to 30.0 in the period. The maximun concentration values between 105.0 and 110.0 μg/m^3, as shown in the framed area. Within the MZ of Poza Rica, "Petroleos Mexicanos" burns gases from the cryogenic plant's gas processing process in a pit burner for long periods of the year, generating concentration value peak readings in the same month of the analysis, but which, in contrast to other years, did not exceed the values reached with dust from the Sahara.

Finally, in **Figure 6(d)** EMCAM1 station, a decrease in $PM_{2.5}$ and concentration readings was observed, compared to 2020 readings; these were below those in 2019, with lower concentrations than 20.0 μg/m^3. This data could be due to a low-pressure channel in southern, as seen in **Figure 5** and **Table 1**. Texas, with data precipitation, and a jet stream rotating above the Gulf of Mexico, promoting the dispersion of particles as seen in **Figure 5**.

The movement of SD from the Yucatan Peninsula, whose $PM_{2.5}$ concentration values are usually similar, is notable since it is the access point for this annual transport. It also shows how the particles moved towards the state of Veracruz through the Coatzacoalcos-Minatitlan area, and upon their arrival in the northern area in the MZ of Poza Rica, they remained for a few days. The observed $PM_{2.5}$ concentrations continued their way and entered the northern states, such as Nuevo León. It was observed that they did not arrive in the same concentration; this could have been due to meteorological phenomena coming from the south of the U.S. and associated with the Gulf of Mexico. **Figure 7(a)** shows that in 2019 and 2020, there were differences between the average $PM_{2.5}$ concentrations of 2.0 μg/m^3.

It was observed that despite being a city with non-industrial activity, maximum values were exceeded in both years. In 2020, values up to 164.0 μg/m^3 were reached. The differences were not significant between the two periods, as seen in the graph, which suggests the recurrent annual entry of SD into the peninsula. **Table 6** shows the station's statistics.

In **Figure 7(b)**, the same behavior was observed in 2020, with higher $PM_{2.5}$ concentration values in the maximum and average values for the years 2018, 2019, and 2020, respectively: 20.0, 23.0, and 24.0 μg/m^3 average. There is a significant difference; the EMCAV2 presents the increasing behavior of $PM_{2.5}$, with values corresponding to 1.0 to 4.0 μg/m^3. This represents an estimated 29% increase when considering the observations of the year 2018 and 7% compared to the year 2019. See **Table 6** for the station statistics calculated in Excel.

Figure 7(c) of EMCAV1 records and shows, according to the observations in **Figure 5**, that the SD occurred between June 25 and 28, reaching higher values in June 2020 as seen in **Figure 7(c)**; the percentage differential values were estimated between 9% and 14% in the 2018 and 2019 concentrations respectively, with very similar mean values but with very large standard deviations in 2018; it is observed that there were a couple of events before the entry of SD, and these values may be due to a particle emission process that is recurrently carried out by the gas processing

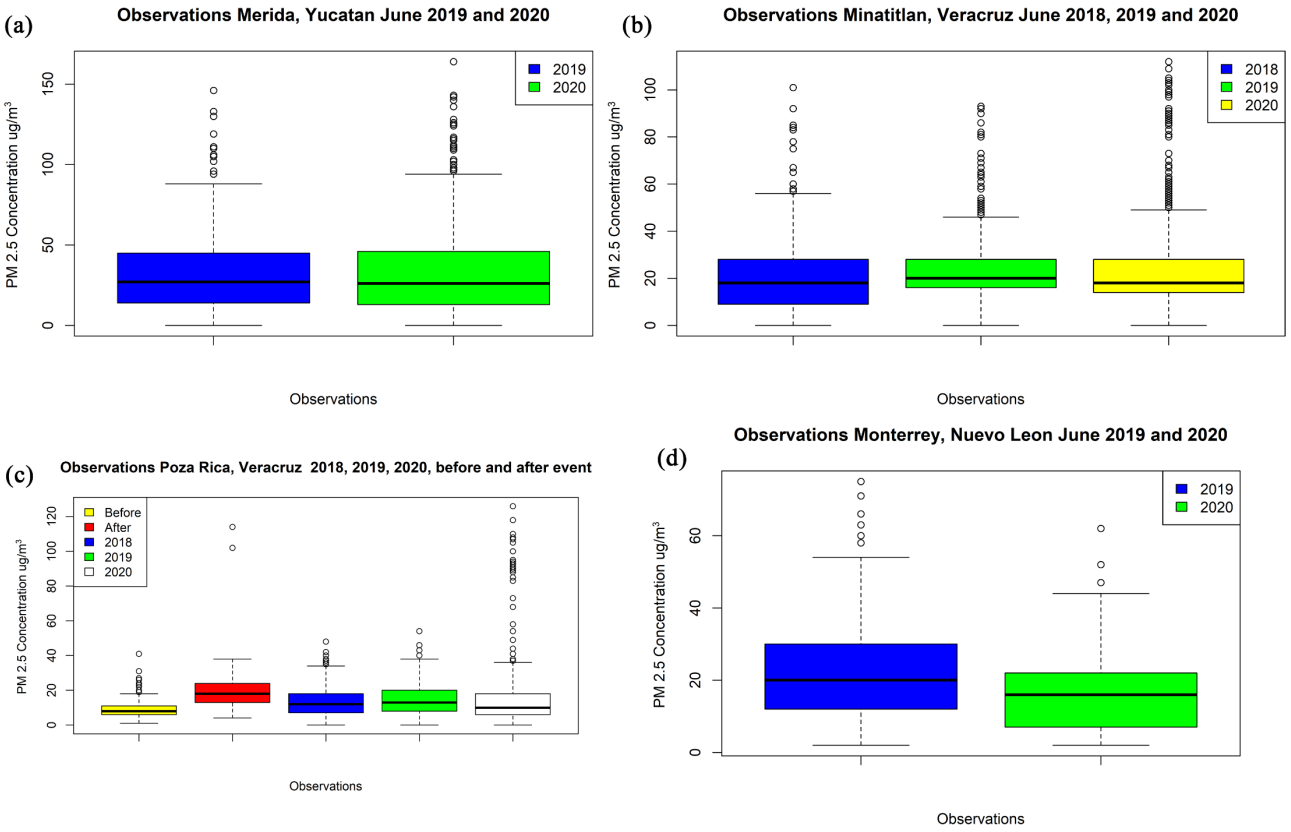


Figure 7. Comparisons of PM2.5 observations for June in 2018, 2019, and 2020 at SEMARNAT air quality stations in the states of Yucatan (EMCAY1), Veracruz (EMCAV1 AND 2), and Nuevo León (EMCAM1).

complex that emits BC particles or to some unidentified factor. It also shows how, before and after the event, concentration changes abruptly. Table 6 shows the station's statistics.

Figure 7(d) of the EMCAM1 station shows concentrations lower than those in 2019. This, as discussed above, could have been due to the meteorological event described above, which reduced $PM_{2.5}$ concentration in the air and promoted its dispersion. See Table 6.

Table 6. Summary of concentration statistics at stations in Yucatan, Veracruz, and Nuevo Leon.

Parameter (mg/m^3)	EMCAY1		EMCAV2			EMCAV1			EMCAM1	
	2019	2020	2018	2019	2020	2018	2019	2020	2019	2020
Average	32.0	33.7	19.5	22.8	23.9	13.0	15.0	15.0	22.0	15.0
Median	27.0	26.0	18.0	20.0	18.0	12.0	13.0	10.0	20.0	16.0
Standard deviation	23.7	29.1	14.3	13.4	18.3	8.0	8.0	18.0	13.0	9.9
Maximum	146.0	164.0	101.0	93.0	112.0	48.0	54.0	126.0	75.0	62.0
Minimum	0.0	0.0	0.0	0.0	0.0	0.0	0.0	0.0	2.0	2.0

As can be seen, the $PM_{2.5}$ concentration values between the stations reviewed

show how, as the SD was transported through the states used to monitor the phenomenon in the day-to-day analysis, the $PM_{2.5}$ concentrations increased and consequently affected air quality in its path, especially in the states of Yucatan and Veracruz. Table 7 shows how the index value changed at station EMCAV1 as it passed through the cities of Poza Rica and Minatitlan.

Table 7 shows the average daily values of PM_{10} and $PM_{2.5}$ in the MZ of Minatitlan and Poza Rica, where it can be observed how, within the study interval from June 25 to 30 and the first 5 days of July, the average concentrations of these parameters increase in such a way that they modify the values of air quality in the comparative cities in the state of Veracruz.

Table 7. Average daily concentrations of PM_{10} and $PM_{2.5}$ in $\mu g/m^3$ in two cities in the state of Veracruz with SEMARNAT air quality monitoring systems.

Date	Concentration in $\mu g/m^3$ $PM_{2.5}$		Concentration in $\mu g/m^3$ PM_{10}
	MZ Poza Rica (1)	MZ Minatitlán (2)	MZ Poza Rica (3)
01/06/20	10	12.4	7.7
02/06/20	5.8	14.2	11.6
03/06/20	7.2	13.0	13.8
04/06/20	5.1	13.3	9.7
05/06/20	6.6	13.0	13.4
06/06/20	9.3	16.7	17.8
07/06/20	9.25	17.6	14.6
08/06/20	14.1	16.0	20.5
09/06/20	18.2	20.5	26.0
10/06/20	13.4	25.0	23.9
11/06/20	5.2	18.3	10.8
12/06/20	6.0	17.7	15.7
13/06/20	10	15.6	28.6
14/06/20	8.3	16.5	22.5
15/06/20	11.5	20.9	22.3
16/06/20	16.0	14.8	20.0
17/06/20	6.0	16.1	11.4
18/06/20	8.0	21.1	15.5
19/06/20	12.1	16.0	14.2
20/06/20	9.0	26.8	15.9
21/06/20	13.0	21.2	20.1
22/06/20	17.2	37.5	38.4
23/06/20	23.6	27.3	51.7

Continued

24/06/20	5.8	28.6	10.2
25/06/20	10.6	38.1	16.9
26/06/20	48.5	93.8	120.3
27/06/20	69.6	55.3	167.1
28/06/20	26.6	36.0	63.7
29/06/20	21.3	34.6	48.8
30/06/20	28.2	34.2	54.9
01/07/20	25.8	35.4	47.0
02/07/20	29.1	32.0	77.3
03/07/20	20.9	22.3	43.6
04/07/20	17.0	24.6	33.4

Note: (1) and (3) ZM Poza Rica, (2) ZM Minatitlán. Source: INECC SINAICA data extracted in 2022.

Figure 8 shows the average daily concentrations in the time series from June 1 to July 4, 2020.

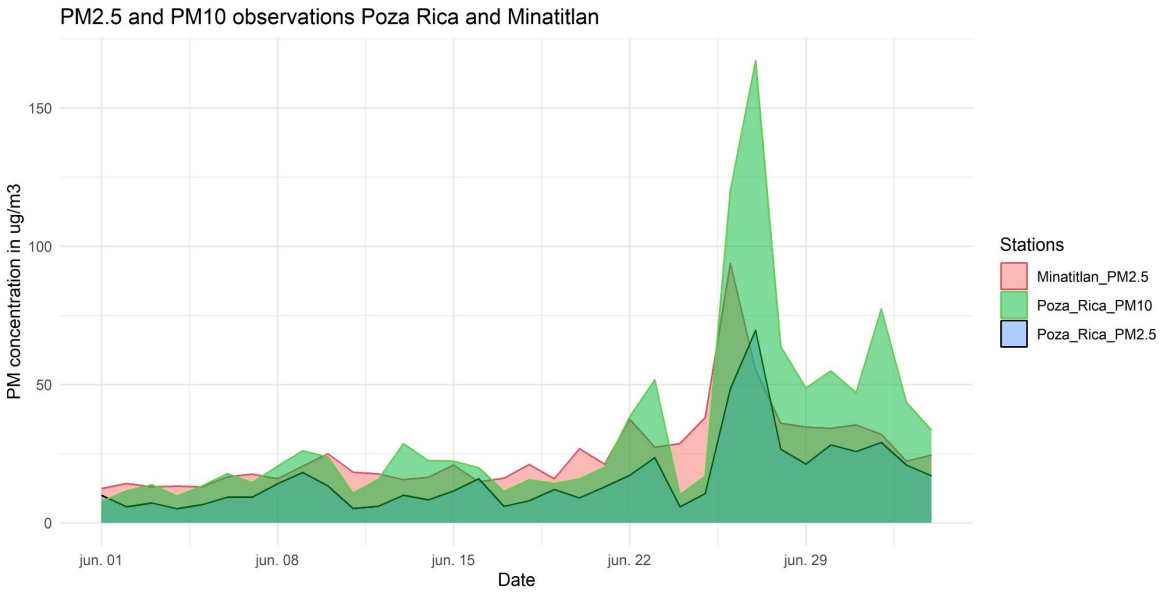


Figure 8. Time series of the average daily concentration of $PM_{2.5}$ and PM_{10} from June 1 to July 5, 2020, during the intrusion of SD in the study area. Source: Authors.

4. Conclusions and Recommendations

In this paper, an analysis was carried out of a phenomenon that annually occurs on planet Earth, which shows us how material from the Sahara Desert in the African continent is transported to various parts of the globe, reaching great distances in Europe, islands in areas such as the Bahamas, Cuba, and the Caribbean in general,

including South, Central, and North America.

Mexico is not an exception, and this SD is usually deposited in the states of the Yucatan Peninsula. However, in June-July 2020, various meteorological phenomena were observed during this period. Mesoscale cyclonic and turbulent systems in the Gulf of Mexico and from the north of the country converged in Mexico. In addition, these promoted a particular transport from the Gulf of Mexico states to the northern states, such as the Nuevo Leon state.

Results from the three starting points of backward trajectories modeled in HYSPLIT show the wind currents from the Saharan Desert, transporting SD during the analysis period in the summer of 2020. The SD was registered in air quality monitoring stations in the states of Yucatan and Veracruz. The winds moved from 5000 to 3000 m AGL from Africa, descending to the Atlantic Ocean until 50 m AGL over Mexico.

The trajectory analyzed by the NASA satellite images in the "Worldview service" coincided with mesoscale cyclonic events that drove the wind from the Caribbean. It was observed that the SD movement along the coast of the Gulf of Mexico from the Yucatan Peninsula to Tabasco and Veracruz reached the states of Tamaulipas and Nuevo Leon. This was driven by temperature changes corresponding to the summer in this area of Mexico. The warm temperature in the Gulf of Mexico promotes winds towards the land, corroborating this trajectory with the HYSPLIT software.

Figure 5 shows a pattern trajectory transport above the coasts in the Gulf of Mexico. It also coincides with precipitation from the EMCAM1 station, where a decrease in PM was observed. The precipitation, together with the phenomena previously indicated, promoted a decrease in $PM_{2.5}$ concentration at that point. Ground-level wind speeds from 11.0 to 14.6 km/h helped to transport the SD. Also, the high summer temperatures promoted turbulent events that transport and diffuse particles on their journey from the south of the country to northern Mexico.

The comparisons between satellite images and backward trajectories in HYSPLIT validated the behavior of $PM_{2.5}$ concentrations used as a parameter for monitoring the SD and PM_{10} evaluated in AQ monitoring stations selected, such as Yucatan (EMCAY1), Veracruz (EMCAV1 and EMCAV2), and Nuevo León (EMCAM1). It was observed that concentrations in $\mu g/m^3$ on the days of the event in June 2020 increased gradually and reached values that exceeded 50.0 $\mu g/m^3$ in many cases.

The values found exceeded Mexican regulations, considering the average concentrations of $PM_{2.5}$ and PM_{10}, and the AHQI calculated. Also, it was found on those days that the AHQI oscillated from bad to extremely bad. There were maximum values in 2020 in EMCAY1 of 101.0 $\mu g/m^3$, EMCAV2 of 112.0 $\mu g/m^3$, EMCAV1 of 126.0 $\mu g/m^3$, and EMCAM1 of 62.0 $\mu g/m^3$. Some aspects of the cities studied show that in the years before the analysis event, there were average values of pollutant concentrations that oscillated from 15.0 to 32.0 $\mu g/m^3$, which, in this summer season and due to their dynamics and location, in addition to natural origin

events such as forest fires, provided a background of particulate emissions, which were exceeded during June 20 to July 4, 2020.

Generally, the EMCAY1 station is affected annually by SD events, as recorded in its AQ station observations. In Minatitlan, in the southern area of Veracruz, at the EMCAV2 station, due to its proximity to the Mexican Gulf coasts, aerosols could be added by the sea breeze. Other emission sources, such as those from the oil-refining industry, could also be involved. At the EMCAV1 station, similarly, the controlled burning of gas from sweetening sour gas emits BC particles, among others, which, added to those emitted by transportation and other natural sources, are recorded daily in the AQ station's observations. We can observe in **Table 7** how the daily average of PM10 before peak days increases from 15.5, 14.2, 15.9, 20.1, 38.4, 51.7, 10.2, 16.9 μg/m^3, and increases until 120.3 and 167.1 μg/m^3, and diminishes after the peak to 63.7, 48.8, 54.9, 47.0, 77.3, 43.6, and 33.4 μg/m^3.

Finally, at the Nuevo León EMCAM1 station, and derived from a meteorological event incoming from the south of the U.S. and the precipitation in the Monterrey area, a decrease in the PM recorded data was observed. At that point, the arrival of SD was lower.

In conclusion, it was found that the annual phenomenon of dust transport from the Sahara Desert is usually recorded in the states of the Yucatan Peninsula; however, mesoscale meteorological conditions and other atmospheric phenomena that raise, transport, and spread this dust to areas of the north and north-northeast of Mexico in states such as Veracruz, Nuevo Leon, or Tamaulipas are not always present. This phenomenon usually displaces it to other areas in the Northern Hemisphere during the summer, such as Barbados and Miami in the U.S., Cuba, and the Caribbean, among other places. The SD transport is not reflected in the inner part of the Gulf of Mexico as it was in this case; it usually affects the south and southeast of Mexico.

The $PM_{2.5}$ and PM_{10} concentrations evaluated affected air quality, so the AHQ indexes changed from poor to extremely poor according to the concentrations recorded and analyzed at stations in the state of Veracruz.

In 2020, the "Niño/Niña" phenomenon increased global temperatures over the sea surfaces and in the air. This season, June and July, had a strong effect on sea and air temperatures. Probably the transport of SD could have been influenced by ENSO.

In future works, tracers could be used to verify the origin of the SD, and this can be extended and analyzed using elemental analysis techniques, metal determinations, chemical components, and finally, to determine the human health impacts.

Acknowledgments

The authors gratefully acknowledge Veracruzana University for the support of this publication. Also, the authors gratefully acknowledge the NOAA Air Resources Laboratory (ARL) for the provision of the HYSPLIT transport and dispersion model and/or the READY website (https://www.ready.noaa.gov) used in

this publication.

A special acknowledgment to Professor Ph.D. Jose Ma Baldasano for his guidance.

Author Contributions

Conceptualization, González-Rocha, S.N. and Cervantes-Pérez, J.; Writing—original draft, González-Rocha, S.N. and Sosa Echeverría, R.; Methodology, González-Rocha, S.N. and Cervantes-Pérez, J.; Formal analysis, González-Rocha, S.N., Sosa Echeverría, R. and Contreras Bermúdez, R.E.; Investigation, González-Rocha, S.N. and Cervantes-Pérez, J.; Project administration, González-Rocha, S.N., Sosa Echeverría, R. and Cervantes-Pérez, J.; Review & editing, Sosa Echeverría, R., Ríos Velasco, L.; Software and visualization, Fuentes García, G., Aguilar-Meléndez, A. and Bauza Mendoza, G.

Conflicts of Interest

The authors declare no conflicts of interest regarding the publication of this paper.

References

[1] Ramírez-Romero, C., Jaramillo, A., Córdoba, M.F., Raga, G.B., Miranda, J., Alvarez-Ospina, H., *et al.* (2021) African Dust Particles over the Western Caribbean—Part I: Impact on Air Quality over the Yucatán Peninsula. *Atmospheric Chemistry and Physics*, **21**, 239-253. https://doi.org/10.5194/acp-21-239-2021

[2] Zhou, L., Gao, C. and Zhang, R. (2023) A Spatiotemporal 3D Convolutional Neural Network Model for ENSO Predictions: A Test Case for the 2020/21 La Niña Conditions. *Atmospheric and Oceanic Science Letters*, **16**, Article ID: 100330. https://doi.org/10.1016/j.aosl.2023.100330

[3] Harr, B., Pu, B. and Jin, Q. (2024) The Emission, Transport, and Impacts of the Extreme Saharan Dust Storm of 2015. *Atmospheric Chemistry and Physics*, **24**, 8625-8651. https://doi.org/10.5194/acp-24-8625-2024

[4] Kaskaoutis, D.G., Nastos, P.T., Kosmopoulos, P.G. and Kambezidis, H.D. (2011) Characterising the Long-Range Transport Mechanisms of Different Aerosol Types over Athens, Greece during 2000-2005. *International Journal of Climatology*, **32**, 1249-1270. https://doi.org/10.1002/joc.2357

[5] Pateraki, S., Assimakopoulos, V.D., Maggos, T., Fameli, K.M., Kotroni, V. and Vasilakos, C. (2013) Particulate Matter Pollution over a Mediterranean Urban Area. *Science of the Total Environment*, **463**, 508-524. https://doi.org/10.1016/j.scitotenv.2013.05.076

[6] Prospero, J.M. and Mayol-Bracero, O.L. (2013) Understanding the Transport and Impact of African Dust on the Caribbean Basin. *Bulletin of the American Meteorological Society*, **94**, 1329-1337. https://doi.org/10.1175/bams-d-12-00142.1

[7] Garrison, V., Foreman, W., Genualdi, S., Griffin, D., Kellogg, C., Majewski, M., *et al.* (2006) Saharan Dust—A Carrier of Persistent Organic Pollutants, Metals and Microbes to the Caribbean. *Revista de Biología Tropical*, **54**, 9-21.

[8] Raga, G.B., Ladino, L.A., Baumgardner, D., Ramirez-Romero, C., Córdoba, F., Alvarez-Ospina, H., *et al.* (2021) ADABBOY: African Dust and Biomass Burning over Yucatan. *Bulletin of the American Meteorological Society*, **102**, E1543-E1556. https://doi.org/10.1175/bams-d-20-0172.1

[9] Córdoba, F., Ramírez-Romero, C., Cabrera, D., Raga, G.B., Miranda, J., Alvarez-Ospina, H., *et al.* (2021) Measurement Report: Ice Nucleating Abilities of Biomass Burning, African Dust, and Sea Spray Aerosol Particles over the Yucatán Peninsula. *Atmospheric Chemistry and Physics*, **21**, 4453-4470. https://doi.org/10.5194/acp-21-4453-2021

[10] Avila, A., Queralt, I., Gallart, F. and Martin-Vide, J. (1996) African Dust over Northeastern Spain: Mineralogy and Source Regions. In: Guerzoni, S. and Chester, R., Eds., *The Impact of Desert Dust across the Mediterranean*, Springer, 201-205. https://doi.org/10.1007/978-94-017-3354-0_19

[11] Bonelli, P., Marcazzan, G.M.B. and Cereda, E. (1996) Elemental Composition and Air Trajectories of African Dust Transported in Northern Italy. In: Guerzoni, S. and Chester, R., Eds., *The Impact of Desert Dust across the Mediterranean*, Springer, 275-283. https://doi.org/10.1007/978-94-017-3354-0_27

[12] Brattich, E., Riccio, A., Tositti, L., Cristofanelli, P. and Bonasoni, P. (2015) An Outstanding Saharan Dust Event at Mt. Cimone (2165 m a.s.l., Italy) in March 2004. *Atmospheric Environment*, **113**, 223-235. https://doi.org/10.1016/j.atmosenv.2015.05.017

[13] Marconi, M., Sferlazzo, D.M., Becagli, S., Bommarito, C., Calzolai, G., Chiari, M., *et al.* (2014) Saharan Dust Aerosol over the Central Mediterranean Sea: PM_{10} Chemical Composition and Concentration versus Optical Columnar Measurements. *Atmospheric Chemistry and Physics*, **14**, 2039-2054. https://doi.org/10.5194/acp-14-2039-2014

[14] Dimitriou, K. and Kassomenos, P. (2018) Day by Day Evolution of a Vigorous Two Wave Saharan Dust Storm—Thermal and Air Quality Impacts. *Atmósfera*, **31**, 105-124. https://doi.org/10.20937/atm.2018.31.02.01

[15] Sprovieri, F., Bencardino, M., Cofone, F. and Pirrone, N. (2011) Chemical Composition of Aerosol Size Fractions at a Coastal Site in Southwestern Italy: Seasonal Variability and Transport Influence. *Journal of the Air & Waste Management Association*, **61**, 941-951. https://doi.org/10.1080/10473289.2011.599267

[16] Dimitriou, K., Remoundaki, E., Mantas, E. and Kassomenos, P. (2015) Spatial Distribution of Source Areas of $PM_{2.5}$ by Concentration Weighted Trajectory (CWT) Model Applied in $PM_{2.5}$ Concentration and Composition Data. *Atmospheric Environment*, **116**, 138-145. https://doi.org/10.1016/j.atmosenv.2015.06.021

[17] Malaguti, A., Mircea, M., La Torretta, T.M.G., Telloli, C., Petralia, E., Stracquadanio, M., *et al.* (2015) Chemical Composition of Fine and Coarse Aerosol Particles in the Central Mediterranean Area during Dust and Non-Dust Conditions. *Aerosol and Air Quality Research*, **15**, 410-425. https://doi.org/10.4209/aaqr.2014.08.0172

[18] Samoli, E., Nastos, P.T., Paliatsos, A.G., Katsouyanni, K. and Priftis, K.N. (2011) Acute Effects of Air Pollution on Pediatric Asthma Exacerbation: Evidence of Association and Effect Modification. *Environmental Research*, **111**, 418-424. https://doi.org/10.1016/j.envres.2011.01.014

[19] Tobías, A., Pérez, L., Díaz, J., Linares, C., Pey, J., Alastruey, A., *et al.* (2011) Short-Term Effects of Particulate Matter on Total Mortality during Saharan Dust Outbreaks: A Case-Crossover Analysis in Madrid (Spain). *Science of the Total Environment*, **412**, 386-389. https://doi.org/10.1016/j.scitotenv.2011.10.027

[20] Urrutia-Pereira, M., Varanda Rizzo, L., Latour Staffeld, P., Chong-Neto, H.J., Viegi, G. and Solé, D. (2021) Dust from the Sahara to the American Continent: Health Impacts. *Allergologia et Immunopathologia*, **49**, 187-194. https://doi.org/10.15586/aei.v49i4.436

[21] Kutralam-Muniasamy, G., Pérez-Guevara, F., Martínez, I.E. and Chari, S.V. (2021) Particulate Matter Concentrations and Their Association with COVID-19-Related Mortality in Mexico during June 2020 Saharan Dust Event. *Environmental Science and*

Pollution Research, **28**, 49989-50000. https://doi.org/10.1007/s11356-021-14168-y

[22] Kaskaoutis, D.G., Kambezidis, H.D., Nastos, P.T. and Kosmopoulos, P.G. (2008) Study on an Intense Dust Storm over Greece. *Atmospheric Environment*, **42**, 6884-6896. https://doi.org/10.1016/j.atmosenv.2008.05.017

[23] Remoundaki, E., Bourliva, A., Kokkalis, P., Mamouri, R.E., Papayannis, A., Grigoratos, T., *et al.* (2011) PM_{10} Composition during an Intense Saharan Dust Transport Event over Athens (Greece). *Science of the Total Environment*, **409**, 4361-4372. https://doi.org/10.1016/j.scitotenv.2011.06.026

[24] Papayannis, A., Mamouri, R.E., Amiridis, V., Kazadzis, S., Pérez, C., Tsaknakis, G., *et al.* (2009) Systematic Lidar Observations of Saharan Dust Layers over Athens, Greece in the Frame of EARLINET Project (2004-2006). *Annales Geophysicae*, **27**, 3611-3620. https://doi.org/10.5194/angeo-27-3611-2009

[25] de Meij, A. and Lelieveld, J. (2011) Evaluating Aerosol Optical Properties Observed by Ground-Based and Satellite Remote Sensing over the Mediterranean and the Middle East in 2006. *Atmospheric Research*, **99**, 415-433. https://doi.org/10.1016/j.atmosres.2010.11.005

[26] Ciardini, V., Di Iorio, T., Di Liberto, L., Tirelli, C., Casasanta, G., di Sarra, A., *et al.* (2012) Seasonal Variability of Tropospheric Aerosols in Rome. *Atmospheric Research*, **118**, 205-214. https://doi.org/10.1016/j.atmosres.2012.06.026

[27] Varga, G., Újvári, G. and Kovács, J. (2014) Spatiotemporal Patterns of Saharan Dust Outbreaks in the Mediterranean Basin. *Aeolian Research*, **15**, 151-160. https://doi.org/10.1016/j.aeolia.2014.06.005

[28] Querol, X., Tobías, A., Pérez, N., Karanasiou, A., Amato, F., Stafoggia, M., *et al.* (2019) Monitoring the Impact of Desert Dust Outbreaks for Air Quality for Health Studies. *Environment International*, **130**, Article ID: 104867. https://doi.org/10.1016/j.envint.2019.05.061

[29] Lenes, J.M., Prospero, J.M., Landing, W.M., Virmani, J.I. and Walsh, J.J. (2012) A Model of Saharan Dust Deposition to the Eastern Gulf of Mexico. *Marine Chemistry*, **134**, 1-9. https://doi.org/10.1016/j.marchem.2012.02.007

[30] Bi, H., Chen, S., Zhang, D., Wang, Y., Kang, L., Alam, K., *et al.* (2024) The Circumglobal Transport of Massive African Dust and Its Impacts on the Regional Circulation in Remote Atmosphere. *Bulletin of the American Meteorological Society*, **105**, E605-E622. https://doi.org/10.1175/bams-d-23-0072.1

[31] NASA. https://worldview.earthdata.nasa.gov/?t=2020-06-26-T19%3A10%3A57Z

[32] Stein, A.F., Draxler, R.R., Rolph, G.D., Stunder, B.J.B., Cohen, M.D. and Ngan, F. (2015) NOAA's HYSPLIT Atmospheric Transport and Dispersion Modeling System. *Bulletin of the American Meteorological Society*, **96**, 2059-2077. https://doi.org/10.1175/bams-d-14-00110.1

[33] Rolph, G., Stein, A. and Stunder, B. (2017) Real-Time Environmental Applications and Display System: READY. *Environmental Modelling & Software*, **95**, 210-228. https://doi.org/10.1016/j.envsoft.2017.06.025

[34] Middleton, N.J. and Goudie, A.S. (2001) Saharan Dust: Sources and Trajectories. *Transactions of the Institute of British Geographers*, **26**, 165-181. https://doi.org/10.1111/1475-5661.00013

[35] Personal Web Repository, Document of CONAFOR. https://www.uv.mx/personal/ngonzalez/data_ojap/

[36] Website of SEMARNAT. https://gisviewer.semarnat.gob.mx/bol/07_2104/

[37] Buchholz, S., Junk, J., Krein, A., Heinemann, G. and Hoffmann, L. (2010) Air Pollution Characteristics Associated with Mesoscale Atmospheric Patterns in Northwest Continental Europe. *Atmospheric Environment*, **44**, 5183-5190. https://doi.org/10.1016/j.atmosenv.2010.08.053

[38] Barkan, J. and Alpert, P. (2010) Synoptic Analysis of a Rare Event of Saharan Dust Reaching the Arctic Region. *Weather*, **65**, 208-211. https://doi.org/10.1002/wea.503

[39] Knippertz, P. and Fink, A.H. (2006) Synoptic and Dynamic Aspects of an Extreme Springtime Saharan Dust Outbreak. *Quarterly Journal of the Royal Meteorological Society*, **132**, 1153-1177. https://doi.org/10.1256/qj.05.109

[40] Pey, J., Querol, X., Alastuey, A., Forastiere, F. and Stafoggia, M. (2013) African Dust Outbreaks over the Mediterranean Basin during 2001-2011: PM_{10} Concentrations, Phenomenology and Trends, and Its Relation with Synoptic and Mesoscale Meteorology. *Atmospheric Chemistry and Physics*, **13**, 1395-1410. https://doi.org/10.5194/acp-13-1395-2013

[41] Varga, G., Kovács, J. and Újvári, G. (2013) Analysis of Saharan Dust Intrusions into the Carpathian Basin (Central Europe) over the Period of 1979-2011. *Global and Planetary Change*, **100**, 333-342. https://doi.org/10.1016/j.gloplacha.2012.11.007

[42] SINAICA Website Database. https://sinaica.inecc.gob.mx/

[43] Meteored Website. https://www.meteored.mx/

[44] INECC Website. https://sinaica.inecc.gob.mx/pags/guias.php